Cyclization of Diazoacetamides Catalyzed by N-Heterocyclic Carbene Dirhodium(II) Complexes

Luis F. R. Gomes,[a] Alexandre F. Trindade,[a] Nuno R. Candeias,[b] Luís F. Veiros,[c] Pedro M. P. Gois,[b] Carlos A. M. Afonso*[a]

[a] CQFM, Centro de Química–Física Molecular, Institute of Nanosciences and Nanotechnology, Instituto Superior Técnico, 1049-001 Lisboa, Portugal

[b] iMed.UL, Faculdade de Farmácia da Universidade de Lisboa, Av. Prof. Gama Pinto, 1649-003 Lisboa, Portugal

[c] CQE, Centro de Química Estrutural, Instituto Superior Técnico, 1049-001 Lisboa, Portugal
Fax +351(21)8464455/7; E-mail: carlosafonso@ist.utl.pt

Received 23 July 2009

Abstract: The axial coordination of N-heterocyclic carbene ligands onto dirhodium(II) complexes was examined, together with its role in the intramolecular C–H insertion reactions of α-diazoacetamides. The formation of a decarbonylated product occurs by a free-carbene mechanism in which the structures of the catalyst and the acetamide play a decisive role.

Key words: carbenoids, carbene complexes, catalysis, diazo compounds, rhodium

The functionalization of saturated C–H bonds is a transformation that is of considerable importance in modern synthetic organic chemistry. The possibility of creating new C–C bonds from nonfunctionalized C–H bonds opens new and exciting possibilities for accessing molecules with complex structures. Among the methods that are available for this transformation, the use of a combination of a diazo compound and a dirhodium(II) complex has emerged as one that gives simple and efficient activation of C–H bonds in both intramolecular and intermolecular reactions.[1–3]

The success that can be achieved by the use of a combination of a diazo compound and a dirhodium(II) complex relies on the reactivity of the resulting metallocarbenes, which are the pivotal intermediates in the activation of nonfunctionalized C–H bonds.[1–3] Such complexes contain a Rh–Rh bond and four bridging ligands that are responsible for controlling the electrophilicity and asymmetry of the catalyst.[1,2] In comparison with the four bridging ligands, the two axial ligands (which are normally solvent molecules) form weaker bonds with the electrophilic center and are thought to play a less important role in catalysis because they are easily displaced.[1,2] Despite this general assumption, we have recently shown that some axial ligands, namely N-heterocyclic carbenes (NHCs), can have a profound impact on the overall reactivity of the complex. The arylation of aldehydes by using boronic acids catalyzed by NHC-dirhodium(II) complexes is a clear example of the ability of axial ligands to influence the reactivity profile of dirhodium(II) complexes.[4]

SYNTHESIS 2009, No. 20, pp 3519–3526
Advanced online publication: 15.09.2009
DOI: 10.1055/s-0029-1217005; Art ID: C03509SS

In line with this observation, we recently showed that these new complexes also have an interesting effect on conventional intramolecular C–H insertion reactions of diazoacetamides.[5] Here, we present our results of studies on the effects of the axial coordination of NHCs in dirhodium(II) complexes and, consequently, on catalytic intramolecular C–H insertion reactions.

N-Heterocyclic carbenes are neutral, two-electron donor (σ-donating) ligands with a small π-back-bonding tendency, and their coordination to dirhodium(II) complexes is occurs essentially through σ-donation from the carbene lone pair to the lowest unoccupied molecular orbital of the dirhodium(II) complex.[6] This is a Rh–Rh antibonding orbital (σ^*) derived from the out-of-phase combination of two z^2 orbitals.[4,7] Thus, the formation of a Rh–NHC bond corresponds to an electron transfer from the carbene to the metallic fragment, and to the population of the Rh–Rh antibonding orbital.[4]

Density functional theory (DFT) calculations[8] performed on dirhodium(II) complexes showed that the length of the Rh–Rh bond increases to 2.46 Å in complexes **4** and **5**, compared with a value of 2.39 Å in the dirhodium complex **1**, which has vacant axial positions. In addition, electron donation from the NHC affects the charge on the metallic fragment, resulting in an increase in the electron density on the terminal rhodium atom as a result of charge transfer through the Rh–Rh bond (Figure 1 and Table 1).

The NHC-dirhodium(II) complexes **4** and **5** display some interesting structural features. They show an almost perfect structural match between the NHC and the dirhodium(II) lantern structure, as the isopropyl groups fit in between the acetoxy bridges, and the carbene ring stays in an eclipsed conformation, thereby providing a high degree of stereoprotection to the rhodium centre, as shown in Figure 2.[4] This arrangement contributes decisively to the stability of the complex under our reaction conditions.[5] This contrasts with the stability of complex **6**, prepared by Snyder et al.,[7] which fragmented in the presence of various diazo substrates. For this reason, the results obtained with complex **6** were identical to those observed when the parent dirhodium(II) complex was used.[7]

On the basis of these results, we examined the cyclization of substrates **7**–**9** with various dirhodium(II) complexes

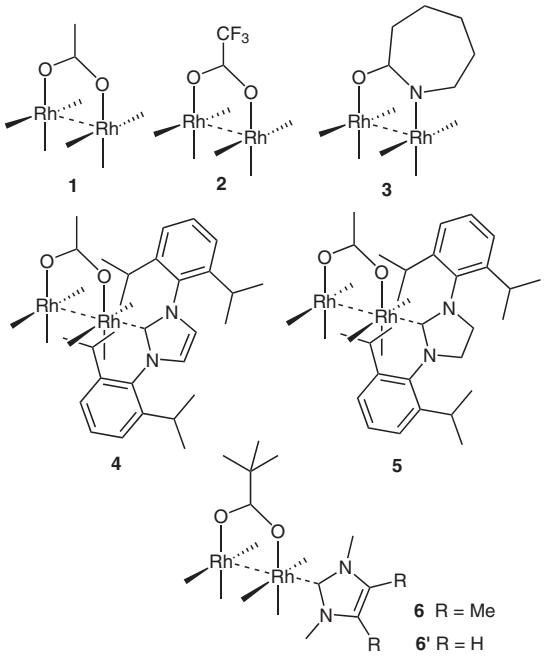

Figure 1 Dirhodium(II) complexes used in the intramolecular C–H insertion reaction of α-diazoacetamides; for clarity, only one of the four bridging ligands in each dirhodium complex is shown

(Table 2). Not surprisingly, the reaction proceeded much more slowly when **4** or **5** were used. This reflects a less favorable nucleophilic attack by the diazo compound on the dirhodium(II) complex as a result of the decreased atomic charge on the terminal Rh centre in complexes **4** and **5**. More important than the impact on the reaction rate was the effect on the cyclization selectivity for these substrates, which are known to afford essentially the γ-lactam isomers **7a**–**9a**. When cyclization of diazoacetamide **7** was performed using catalysts **4** and **5**, the yield of the γ-lactam isomer decreased and some β-lactam **7b** was formed (Table 2, entries 1–5). More importantly, a new decarbonylated product **7c** was isolated (Table 2, entries 4 and 5). Traces (less than 2%) of this product could also be found in the crude reaction mixture when using complex

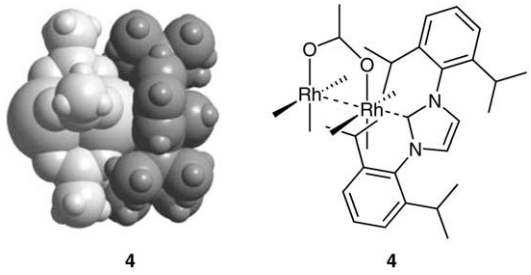

Figure 2 Optimized geometry for the $Rh_2(OAc)_4$(NHC) complex **4** (left; the NHC ligand is darkened); for clarity, only one of the four bridging acetyl groups in the dirhodium complex is shown in the structural diagram

3, but no decarbonylation products were formed with any of the other catalysts, nor were they observed in our recent studies on UV-promoted cyclization reactions of diazoacetamides (Table 2, entry 6).[9] With regard to the other diazoacetamides shown in Scheme 1, liberation of carbon monoxide was more pronounced in substrate **8**, which has a more electron-withdrawing α-substituent, whereas the sulfonyl-diazoacetamide **9** gave a rather complex mixture in which the decarbonylation product was not identified.

These results confirmed the influence of both the catalyst and diazoacetamide structure on the occurrence of a decarbonylation mechanism. We therefore examined the cyclization reactions of various diazoacetamides catalyzed by **4** and/or **5** (Scheme 1, Tables 3 and 4). In general these substrates afforded the expected lactams without forming the decarbonylation product. Interestingly, in the case of the substrate **10**, the cyclization was even more selective than when dirhodium tetracetate was used.

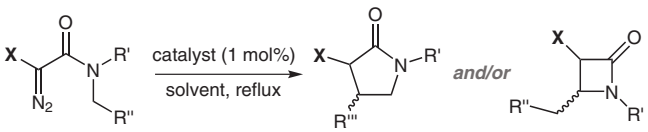

Scheme 1 Cyclization of various diazocetamides using complexes **1**, **4**, and **5**

Table 1 DFT-Calculated[a] Data for Dirhodium Complexes **1**–**6′** and **20**

Entry	Complex	Atomic Charge[b] ($Rh_{Terminal}$)	Atomic Charge[b] (Rh_{NHC})	$d_{Rh–Rh}$ (Å)	$WI_{Rh–Rh}$[c]	$d_{C(NHC)–Rh}$ (Å)	$WI_{C(NHC)–Rh}$[c]
1	**1**	0.93	0.93	2.39	0.79	–	–
2	**2**	0.95	0.95	2.39	0.80	–	–
3	**3**	0.81	0.81	2.39	0.76	–	–
4	**4**	0.75	0.92	2.46	0.54	2.17	0.38
5	**5**	0.76	0.92	2.46	0.54	2.18	0.38
6[d]	**6′**	0.71	0.88	2.44	0.49	2.08	0.44
7	**20**	0.77	0.92	2.45	0.56	2.20	0.35

[a] DFT calculations were performed at the B3LYP/631LAN level of theory.
[b] Natural population analysis charge.
[c] WI = Wiberg index.
[d] Calculations performed at the B3PW91/631LAN level using complex **6′** as a model.

Table 2 Cyclization of Diazoacetamides **7–9** by Using Complexes **1–5**

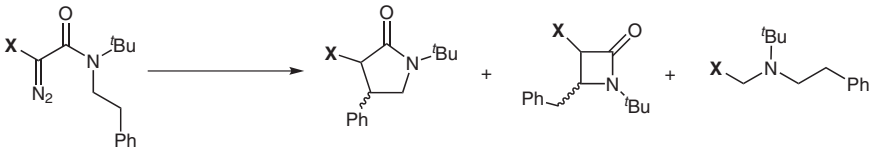

7 X = $PO(OEt)_2$
8 X = COMe
9 X = SO_2Ph

7a X = $PO(OEt)_2$
8a X = COMe
9a X = SO_2Ph

7b X = $PO(OEt)_2$
8b X = COMe
9b X = SO_2Ph

7c X = $PO(OEt)_2$
8c X = COMe

Entry	Substrate (amount)	Catalyst (amount)	Conditions	Yield (%) of **7a–9a**[a]	*cis/trans*[b]	Yield (%) of **7b–9b**	*cis/trans*[b]	Yield (%) of **7c–8c**[a]
1	**7** (0.3 mmol)	**1** (1 mol%)	DCE (0.1 M), reflux, 4 h	81 (91)	0.06:1	(5)	2.1:1	–
2	**7** (0.157 mmol)	**2** (1 mol%)	DCE (0.1 M), reflux, 12 h	66 (82)	0.02:1	10 (11)	3.9:1	–
3	**7** (0.157 mmol)	**3** (1 mol%)	DCE (0.1 M), reflux, 7 h	76 (80)	0.09:1	3 (3)	2.3:1	0 (<2)
4	**7** (0.3 mmol)	**4** (1 mol%)	DCE (0.1 M), reflux, 46 h	56 (60)	0.07:1	7 (9)	2.7:1	23 (25)
5	**7** (0.3 mmol)	**5** (1 mol%)	DCE (0.1 M), reflux, 24 h	66 (79)	0.06:1	7 (8)	2.6:1	9 (9)
6	**7** (0.103 mmol)	–	*hν*,[c] hexanes (1 mL), 8.5 h	64 (66)	1:1	–	–	–
7	**8** (0.3 mmol)	**1** (1 mol%)	DCE (0.03 M), reflux, 6 h	47 (65)	0:1	25 (34)	0:1	–
8	**8** (0.3 mmol)	**4** (1 mol%)	DCE (0.03 M), reflux, 6 h	17 (18)	0:1	35 (46)	0:1	– (36)
9	**8** (0.3 mmol)	**5** (1 mol%)	DCE (0.03 M), reflux, 6 h	18 (32)	0:1	14 (39)	0:1	– (29)
10[12]	**9** (1.0 mmol)	**1** (2.5 mmol)	CH_2Cl_2, reflux, 12 h	95	0:1	–	–	–
11	**9** (0.3 mmol)	**4** (2.5 mol%)	CH_2Cl_2 (0.1 M), reflux, 53 h	67 (89)	0:1	5 (8)	0:1	–
12	**9** (0.3 mmol)	**5** (2.5 mol%)	DCE (0.1 M), reflux, 4 h	54 (64)	0:1	21 (30)	0:1	–

[a] Isolated yields; the conversion determined by ^{31}P NMR or ^{1}H NMR spectroscopy of the crude mixture is given in parentheses.
[b] The *cis/trans* ratios were determined by ^{31}P NMR or ^{1}H NMR spectroscopy on the crude mixture.
[c] UV irradiation (Hg lamp, Hanau TQ150).

Table 3 Products from the Cyclization of Various Diazocetamides Using Complexes **1**, **4**, and **5** According to Scheme 1

Catalyst, amount (mol%)	Solvent (concn)	Diazo compd (mmol)	Temp[a]	Time (h)	Product, yield (%)[b]	
					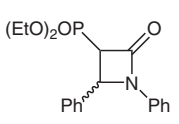 **10b**	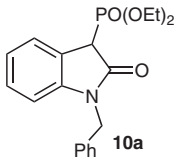 **10a**
1 (1 mol%)[10]	DCE (0.1 M)	0.150 mmol		24	(12)	(83)
4 (1 mol%)	DCE (0.1 M)	0.130 mmol		53	6 (7)	80 (90)
5 (1 mol%)	DCE (0.1 M)	0.130 mmol		53	12 (12)	76 (85)
					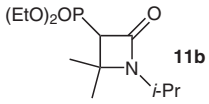 **11b**	
1 (1 mol%)	CH_2Cl_2 (0.09 M)	0.50 mmol		6.5	88 (99)	
5 (1 mol%)	CH_2Cl_2 (0.09 M)	0.126 mmol		21	80 (88)	
					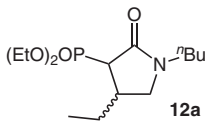 **12a**	
1 (1 mol%)	DCE (0.1 M)	0.30 mmol		2	87 (92)	
5 (1 mol%)	DCE (0.1 M)	0.126 mmol		16	89 (93) *cis/trans* = 0.07:1	

Table 3 Products from the Cyclization of Various Diazocetamides Using Complexes **1**, **4**, and **5** According to Scheme 1 (continued)

Catalyst, amount (mol%)	Solvent (concn)	Diazo compd (mmol)	Temp[a]	Time (h)	Product, yield (%)[b]
					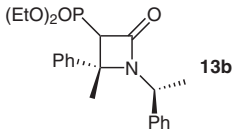 **13b**
1 (1 mol%)	DCE (0.08 M)	0.150 mmol		1.5	56 (77) *cis*/*trans* = 1:1.2
5 (1 mol%)	DCE (0.08 M)	0.118 mmol		47	53 (73) *cis*/*trans* = 0.74:1
					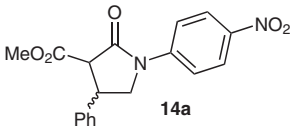 **14a**
1 (2 mol%)	CH_2Cl_2 (0.26 M)	0.360 mmol	r.t.	17	98 *cis*/*trans* = 0:1
5 (1 mol%)	DCE (0.08 M)	0.128 mmol	reflux	24	98 *cis*/*trans* = 0:1
					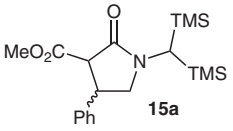 **15a**
1 (2 mol%)	CH_2Cl_2 (0.2 M)	0.180 mmol		1.25	93 (>97%) *cis*/*trans* = 0:1
5 (2 mol%)	CH_2Cl_2 (0.2 M)	0.119 mmol		20	95 (>97%) *cis*/*trans* = 0:1

[a] Unless otherwise indicate, all reactions were carried out under reflux.
[b] Isolated yields; the conversion determined by ^{31}P NMR or ^{1}H NMR spectroscopy of the crude mixture is given in parentheses.

A surprisingly different result was obtained, however, when the cyclization of asymmetric diazoacetamide **16** was promoted by NHC-dirhodium(II) catalysts **4** and **5**. In this case, the decarbonylation product was obtained in up to 47% yield (Table 4).

The formation of phosphonate **16c** appears to result from a delicate balance between stereoelectronic effects of the diazoacetamide and phosphonate groups, since no decarbonylation product was detected by ^{1}H NMR spectroscopy for the crude reaction product from the sulfonyl diazoacetamide **17**. This idea was reinforced by the cy-

Table 4 Cyclization of Asymmetric Diazoacetamide **16** and **17**

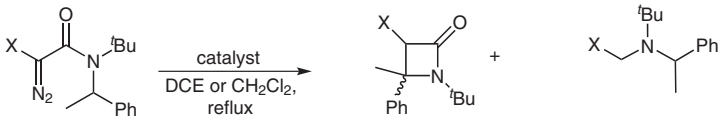

16 X = $PO(OEt)_2$
17 X = SO_2Ph

16b X = $PO(OEt)_2$
17b X = SO_2Ph

16c X = $PO(OEt)_2$
17c X = SO_2Ph

Entry	Diazo compound (amount)[a]	Catalyst (amount)	Time (h)	Yield of β-lactam (%)[b]	*cis*/*trans*	Yield of amine (%)[b]
1[11]	**16** (5.25 mmol)	**1** (1 mol%)	4	77	1.5:1	–
2	**16** (0.140 mmol)	**4** (1 mol%)	25	15 (19)	0.44:1	47 (57)
3	**16** (0.140 mmol)	**5** (1 mol%)	25	17 (23)	0.63:1	44 (51)
4	**16** (0.052 mmol)	**1** (2 mol%) + **4** (2 mol%)	3	56 (72)	1.38:1	13 (18)
5	**17** (0.128 mmol)	**1** (2.5 mol%)	2.5	33 (39)	–[c]	–
6	**17** (0.128 mmol)	**4** (2.5 mol%)	120	51 (60)	–[c]	–
7	**17** (0.128 mmol)	**5** (2.5 mol%)	120	52 (60)	–[c]	–

[a] All reactions were carried out in DCE (entries 1–4) or in CH_2Cl_2 (entries 5–7) (0.1 M).
[b] Isolated yields; the conversion determined by ^{31}P NMR or ^{1}H NMR spectroscopy of the crude mixture is given in parentheses.
[c] Only one isomer was observed.

clization of diazoacetamide **18**, which again did not afford the decarbonylated product, despite its structure similarity to substrate **16** (Scheme 2).

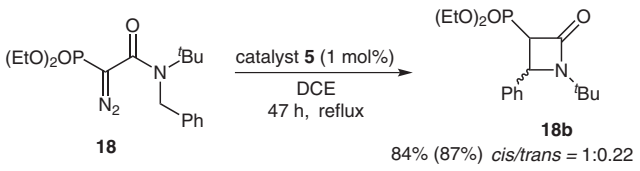

Scheme 2 Cyclization of asymmetric diazoacetamide **18**

Despite a lower free-electron density at the coordination site and, consequently, a lower reaction rate, catalyst **4** can still compete with dirhodium tetraacetate for the decomposition of substrate **16**, affording 18% of the decarbonylated product **16c** in a competitive reaction when both catalysts **1** and **4** are present in the reaction medium (Table 4, entry 4).

The results of our calculations show that catalysts **4** and **5** are very similar in terms of their electronic and physical structures (Table 1); however, their catalytic activities show some differences. For example, complex **4** appears to be more prone to give product **16c**. We therefore decided to prepare a new complex with chloride groups attached to the NHC backbone to examine the effect of electronic effects of the NHC on the selectivity of the reaction (Scheme 3). Complex **20** was obtained in 85% yield by treating the NHC **19**[13] with dirhodium tetraacetate.

The atomic charge calculated for the terminal rhodium atom in complex **20** is similar to those of **4** and **5**, but the C(NHC)–Rh bond is slightly longer and weaker in complex **20** (Table 1). This is confirmed by the corresponding Wiberg index, which in complex **20** is 0.35, whereas it is 0.38 in complexes **4** and **5**; this is probably due to the inductive effect exerted by the two chlorine atoms in **20** (Scheme 3). Surprisingly complex **20** proved to be the best complex to induce the formation of the decarbonylated product **16c**, which was obtained with 61% conversion (Scheme 4).

To study the mechanism of the decarbonylation reaction, we examined the decomposition of **16** with complex **4** in 1,2-dichloroethane saturated with deuterium oxide and in deuterated 1,2-dichloroethane, as shown in Scheme 5. The reaction in the presence of deuterium oxide resulted in incorporation of deuterium in the decarbonylated product, whereas no incorporation was detected when deuterated 1,2-dichloroethane was used as the only solvent. Additionally, no incorporation of deuterium was observed on standing the amine **16c** in a 2.3:1 mixture of tetrahydrofuran and deuterium oxide at 55 °C for 27 h. These experiments showed that a Wolff mechanism may be involved in the generation of **16c**; this was corroborated by the fact that when diazoacetamide **16** was thermally decomposed in refluxing 1,2-dichloroethane it gave product **16c** in 33% yield together with 17% of the corresponding β-lactam.

By considering these results, we hypothesized that the presence of a σ-donating NHC ligand could weaken the bond between the carbene and the terminal rhodium centre. In fact, DFT analysis of these two structures con-

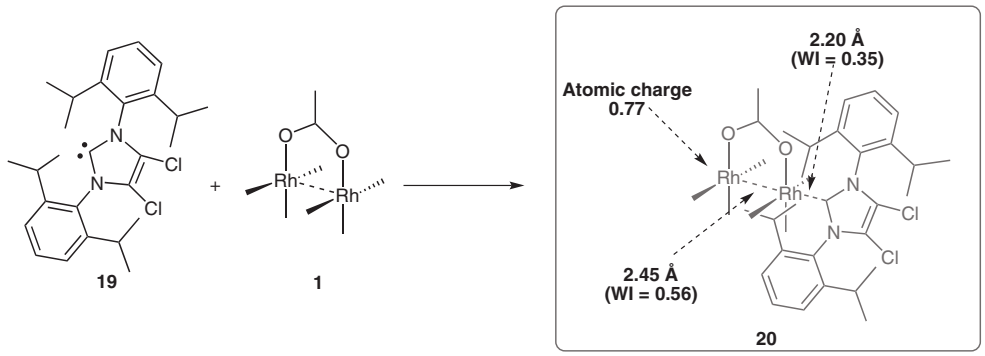

Scheme 3 Synthesis of complex **20** and some relevant structural and electronic calculated data; for clarity, only one of the four bridging acetyl ligands in each of the dirhodium complexes is shown.

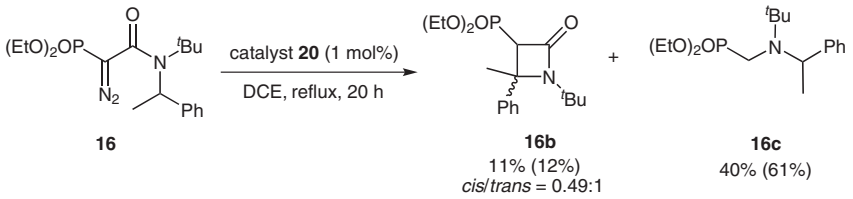

Scheme 4 Effect of catalyst **20** on the formation of product **16c**. *Reagents and conditions*: diazo compound (0.121 mmol), DCE (0.1 M), and catalyst (1 mol%).

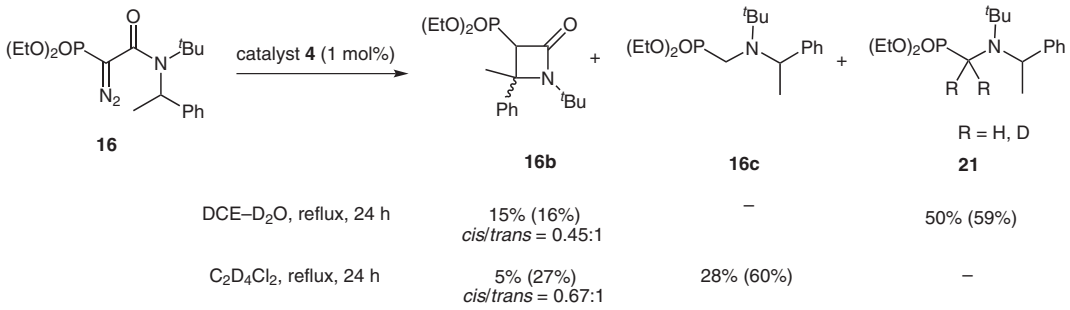

Scheme 5 Decomposition of diazoacetamide **16** with catalyst **4** in deuterated solvents

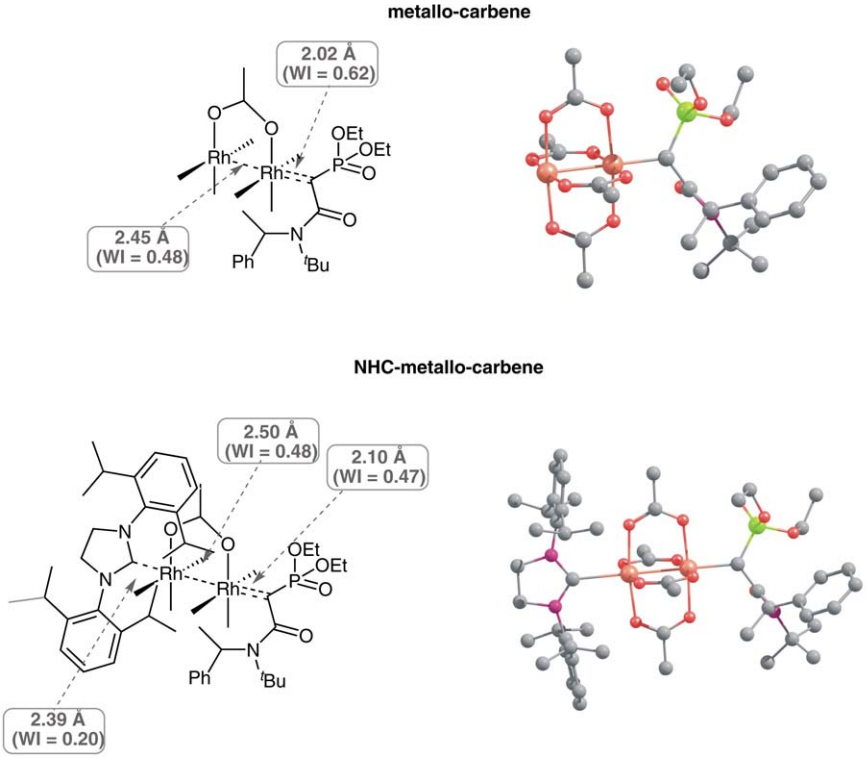

Figure 3 Relevant structural and electronic parameters calculated for the metallo-carbene and NHC-metallo-carbene derived from diazo compound **16**

firmed this effect, as the rhodium–carbene bond became 0.08 Å longer as a result of the presence of the axial ligand, as shown in Figure 3.

Taking the experimental and theoretical results together, we hypothesized that the effect of the NHC relies on the possibility that this ligand can participate in a push–pull mechanism. As shown in Scheme 6, the reaction of the NHC-dirhodium(II) with the diazo species forms the metallo-carbene. In this species, the presence of the Rh=C_{diazo} bond weakens the Rh–C_{NHC} bond (pull), although the integrity of the bond is, to some extent, secured by the stereochemical protection conferred by the structure of the NHC. On the other hand, the NHC also weakens the metallo-carbene (push), which, in combination with the stereochemical effects exerted by the acetamide structure, may lead to the generation of a free carbene-type intermediate that undergoes a typical Wolff rearrangement to form the decarbonylated product.

In conclusion, we have shown that axial coordination of NHC ligands in dirhodium(II) complexes can have an important effect on the rates and selectivities of intramolecular reactions. Most importantly, the possibility of the NHC engaging in a push–pull mechanism favors the generation of a free carbene-type intermediate that affords a decarbonylated product. In addition to this effect, the diazoacetamide structure also contributes decisively to this reaction pathway.

DCE, toluene, DME, PhCl, Et_3N, and CH_2Cl_2 were distilled over CaH under argon. THF was distilled over Na/benzophenone. TsN_3 was prepared from TsCl and NaN_3.[14] NaH was used as a 55% dispersion in mineral oil. DCE-d_4 and D_2O were acquired from Cambridge Isotope Laboratories. $Rh_2(OAc)_4$ and $Rh_2(TFA)_4$ were obtained from Aldrich. Catalysts **3**,[15] **4**,[4b] and **5**[4b] were prepared as previously described. All reactions were carried out under argon. Flash chromatography was carried out on silica gel [Merck (Ref. 109385) or Scharlau (230–400 mesh ASTM)], neutral alumina [Macherey-Nagel (Ref. 815020)] or basic alumina [Macherey-

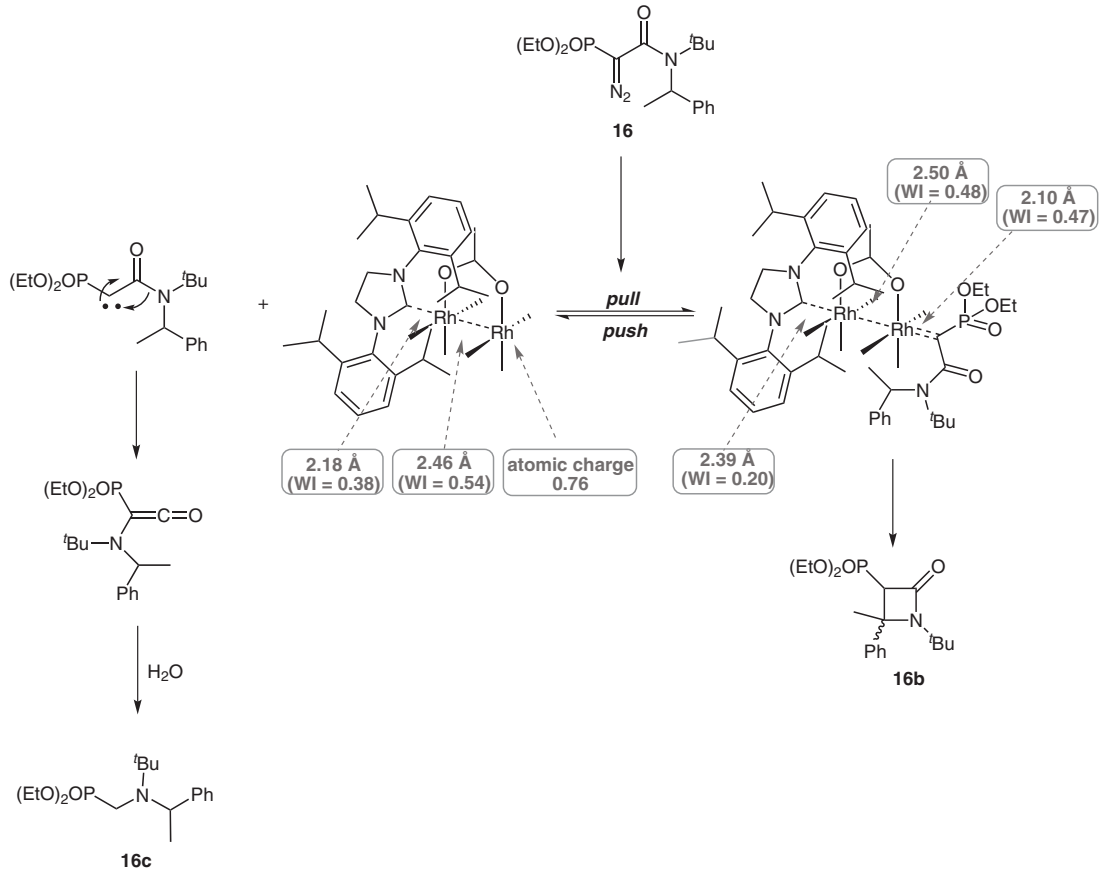

Scheme 6 Proposed mechanism for the decomposition of diazoacetamide **16**

Nagel (Ref. 815010, activity 1)]. Preparative TLC was carried out on silica [Merck 60 G F_{254} (Ref. 105788)] or alumina [Merck 60 F_{254} (Ref. 107730)]. Reaction mixtures were analyzed by TLC on silica 60 F_{254} [Merck (ref. 105554)] or neutral alumina [60 F_{254}, Merck (ref. 105550)]; spots were visualized by UV irradiation and phosphomolybdic acid soln or I_2. IR spectra were recorded with a Jasco FT/IR-430 model as thinly dispersed films on NaCl. High- and low-resolution mass spectra (EI, FAB$^+$) were recorded by the mass spectrometry service of the University of Santiago de Compostela (Spain). NMR spectra were recorded with a Bruker Ultrashield Avance II 400 or 300 in toluene-d_8 or $CDCl_3$ as solvents and TMS as an external standard for ^{1}H and ^{13}C, and H_3PO_4 as an external standard for ^{31}P NMR. All coupling constants are expressed in Hz.

α-Diazoacetamides and products were obtained as previously described,[5] except for **17**, which was obtained following a general procedure used previously.[12] Substrates **11**,[11] **13**,[9] **14**,[16] and **15**,[17] and products **11b**,[11] **13b**,[9] **14a**,[16]and **15a**,[17] have already been reported elsewhere.

Dirhodium Complex 20

A flame-dried Schlenk tube was charged with a suspension of $Rh_2(OAc)_4$ (50 mg, 0.11 mmol) in freshly distilled and dried toluene (4 mL). Carbene **19**[13] (103 mg, 0.23 mmol) was added, and the mixture was heated at 80 °C until the soln turned the color of red wine (about 2 h). The soln was concentrated, and the residue was purified by chromatography (30% EtOAc–hexane) to give a purple-bluish powder; yield: 85%.

^{1}H NMR (toluene-d_8): δ = 7.13–6.99 (m, toluene), 3.29–3.24 (m, 4 H), 2.15–2.12 (toluene), 1.34 (br s, 12 H), 1.25 (d, J = 6.6 Hz, 12 H), 1.08 (d, J = 6.6 Hz, 12 H).

^{13}C NMR (toluene-d_8): δ = 188.57, 146.27, 137.40, 134.51, 129.68, 123.25, 119.23, 28.33, 23.91, 23.41, 22.70.

MS (FAB$^+$): m/z = 897.9 [M$^+$], 457.1.

HRMS (FAB$^+$): m/z calcd for $C_{35}H_{46}Cl_2N_2O_8Rh_2$, 898.0741; found, 898.0745.

Dirhodium(II)-Catalyzed Decomposition of α-Diazoacetamides; General Procedure

A soln of the α-diazoacetamide in the anhyd chlorinated solvent was added to the catalyst under argon. The soln was magnetically stirred under reflux until the substrate was consumed (TLC). The solvent was evaporated under reduced pressure, and a NMR spectrum was recorded to determine the relative product ratio. The crude mixture was purified by chromatography (silica or alumina).

Reactions with Deuterated Solvents; General Procedures

Diazo decomposition in wet DCE: DCE (3 mL) and D_2O (300 μL) were equilibrated for 11 days before the organic phase (1.4 mL) was used in the reaction with the diazo compound (0.117 mmol) and catalyst (1 mol%).

Diazo decomposition in 1,2-dichloroethane-d_4: A sealed glass ampoule containing the a mixture of the diazo compound (0.143 mmol), DCE-d_4 (0.266 g), and catalyst (1 mol%) under argon was introduced into a glass reactor containing DCE and heated at 85 °C for 24 h. The ampoule was then opened, the solvent was evaporated under reduced pressure, and a NMR spectrum was recorded to determine the relative product ratio. The crude mixture was purified by chromatography (alumina).

N-tert-Butyl-*N*-(1-phenylethyl)-2-(phenylsulfonyl)acetamide

This precursor of substrate **17** was prepared by following general reported procedure,[12] starting from 2-methyl-*N*-(1-phenylethyl)propan-2-amine[11] (0.694 g, 3.92 mmol) as a white solid; yield: 0.739 g (53%, two steps); mp 85–87 °C; R_f = 0.36 (EtOAc–hexanes, 3:7).

IR (film): 2976, 1651, 1321, 1157, 725 cm^{-1}.

^1H NMR (400 MHz, $CDCl_3$): δ = 1.55 [s, 9 H, NC(CH_3)$_3$], 1.85 (d, *J* = 6.8 Hz, 3 H, CH_3CHN), 3.59 (d, *J* = 14.4 Hz, 1 H, SO_2*H*HCO), 3.90 (d, *J* = 14.8 Hz, 1 H, SO_2H*H*CO), 5.12 (q, *J* = 6.8 Hz, 1 H, CH_3C*H*N), 7.29–7.32 (m, 3 H, Ar), 7.38–7.41 (m, 2 H, Ar), 7.50–7.54 (m, 2 H, Ar), 7.61–7.65 (m, 1 H, Ar), 7.81–7.83 (m, 2 H, Ar).

^{13}C NMR (100 MHz, $CDCl_3$): δ = 21.32 (*C*H_3CHPh), 29.04 [NC(*C*H_3)$_3$], 52.66 (CH_3*C*HPh), 59.87 [N*C*(CH_3)$_3$], 63.38 (SO_2*C*H_2CO), 125,57, 127.20, 128.72, 128.81, 129.26, 133.57, 139.92 (q), 142.87 (q) (Ar), 164.01 (CO).

_N_-*tert*-Butyl-2-diazo-_N_-(1-phenylethyl)-2-(phenylsulfonyl)acetamide (17)

The α-diazoacetamide **17** was prepared by following the reported general procedure,[12] starting from the acetamide precursor (0.516 g, 1.44 mmol), and obtained as a yellow solid; yield: 0.331 g (60 %); R_f = 0.79 (EtOAc–hexanes, 3:7).

IR (film): 2976, 2091, 1643, 1333, 729 cm^{-1}.

^1H NMR (400 MHz, $CDCl_3$): δ = 1.40 [s, 9 H, NC(CH_3)$_3$], 1.86 (d, *J* = 7.2 Hz, 3 H, CH_3CHN), 5.11 (q, *J* = 7.2 Hz, 1 H, CH_3C*H*N), 7.30–7.33 (m, 1 H, Ar), 7.37–7.40 (m, 4 H, Ar), 7.54–7.58 (m, 2 H, Ar), 7.62–7.66 (m, 1 H, Ar), 7.99–8.01 (m, 2 H, Ar).

^{13}C NMR (100 MHz, $CDCl_3$): δ = 20.13 (*C*H_3CHPh), 29.22 [NC(*C*H_3)$_3$], 55.56 (CH_3*C*HPh), 59.80 [N*C*(CH_3)$_3$], 126.90, 127.44, 127.90, 128.64, 128.97, 133.48, 141.60 (q), 142.36 (q) (Ar), 162.37 (CO).

1-*tert*-Butyl-4-methyl-4-phenyl-3-(phenylsulfonyl)azetidin-2-one (17b)

White solid; mp 134–138 °C; R_f = 0.18 (EtOAc–hexanes, 1:4).

IR (film): 2980, 1751, 1319, 1150, 1084 cm^{-1}.

^1H NMR (400 MHz, $CDCl_3$): δ = 1.37 [s, 9 H, NC(CH_3)$_3$], 2.52 [s, 3 H, CH_3C(Ph)N], 4.24 (s, 1 H, SO_2C*H*CO), 7.34–7.47 (m, 3 H, Ar), 7.49–7.51 (m, 2 H, Ar), 7.55–7.59 (m, 2 H, Ar), 7.64–7.71 (m, 1 H, Ar), 8.04–8.07(m, 2 H, Ar).

^{13}C NMR (100 MHz, $CDCl_3$): δ = 20.12 [*C*H_3C(Ph)N], 28.41 [NC(*C*H_3)$_3$], 56.76 [N*C*(CH_3)$_3$], 65.24 [CH_3*C*(Ph)N], 79.60 [SO_2*C*HCO], 125.35, 128.28, 128.90, 129.00, 129.08, 134.19, 139.88 (q), 142.92 (q) (Ar), 159.39 (CO) ppm.

An ORTEP plot of the X-ray crystal structure is available in the supporting information.

Supporting Information for this article is available online at http://www.thieme-connect.de/ejournals/toc/synthesis.

Acknowledgment

We thank to Fundação para a Ciência e Tecnologia (POCI 2010) and FEDER (PTDC/QUI/66695/2006, PTDC/QUI/66015/2006, SFH/BPD/46589/2008 and SFRH/BD/30619/2006) for their financial support, and the Portuguese NMR Network (IST-UTL Center) for providing access to the NMR facility.

References

(1) (a) Doyle, M. P.; McKervey, M. A.; Ye, T. *Modern Catalytic Methods for Organic Synthesis with Diazo Compounds: From Cyclopropanes to Ylides*; Wiley: New York, **1998**. (b) Lou, Y.; Remarchuk, T. P.; Corey, E. J. *J. Am. Chem. Soc.* **2005**, *127*, 14223. (c) Cotton, F. A.; Hillard, E.; Murillo, C. A. *J. Am. Chem. Soc.* **2002**, *124*, 5658. (d) Zhang, Z.; Wang, J. *Tetrahedron* **2008**, *64*, 6577.

(2) (a) Davies, H. M. L.; Beckwith, R. E. *Chem. Rev.* **2003**, *103*, 2861. (b) Doyle, M. P. *J. Org. Chem.* **2006**, *71*, 9253. (c) Gois, P. M. P.; Afonso, C. A. M. *Eur. J. Org. Chem.* **2004**, 3773.

(3) For selected examples, see: (a) Catino, A. J.; Forslund, R. E.; Doyle, M. P. *J. Am. Chem. Soc.* **2005**, *126*, 13622. (b) Catino, A. J.; Nichols, J. M.; Choi, H.; Gottipamula, S.; Doyle, M. P. *Org. Lett.* **2005**, *7*, 5167. (c) Liang, C.; Peillard, F. R.; Fruit, C.; Müller, P.; Dodd, R. H.; Dauban, P. *Angew. Chem. Int. Ed.* **2006**, *45*, 4641. (d) Reddy, R. R.; Davies, H. M. L. *Org. Lett.* **2006**, *8*, 5013. (e) Fiori, K. W.; Du Bois, J. *J. Am. Chem. Soc.* **2007**, *129*, 562. (f) Anada, M.; Tanaka, M.; Washio, T.; Yamawaki, M.; Abe, T.; Hashimoto, S. *Org. Lett.* **2007**, *9*, 4559. (g) Doyle, M. P.; Valenzuela, M.; Huang, P. *Proc. Natl. Acad. Sci. U.S.A.* **2004**, *101*, 5391. (h) Anada, M.; Washio, T.; Shimada, N.; Kitagaki, S.; Nakajima, M.; Shiro, M.; Hashimoto, S. *Angew. Chem. Int. Ed.* **2004**, *43*, 2665. (i) Forslund, R. E.; Cain, J.; Colyer, J.; Doyle, M. P. *Adv. Synth. Catal.* **2005**, *347*, 87. (j) Washio, T.; Nakamura, S.; Anada, M.; Hashimoto, S. *Heterocycles* **2005**, *66*, 567. (k) Wang, Y.; Wolf, J.; Zavalij, P.; Doyle, M. P. *Angew. Chem. Int. Ed.* **2008**, *47*, 1439. (l) Catino, A. J.; Nichols, J. M.; Gorslund, R. E.; Doyle, M. P. *Org. Lett.* **2005**, *7*, 2787. (m) Gois, P. M. P.; Candeias, N. R.; Afonso, C. A. M. *J. Mol. Catal. A: Chem.* **2005**, *227*, 17.

(4) (a) Gois, P. M. P.; Trindade, A. F.; Veiros, L. F.; Andre, V.; Duarte, M. T.; Afonso, C. A. M.; Caddick, S.; Cloke, F. G. N. *Angew. Chem. Int. Ed.* **2007**, *46*, 5750. (b) Gois, P. M. P.; Trindade, A. F.; Veiros, L. F.; Andre, V.; Duarte, M. T.; Afonso, C. A. M.; Caddick, S.; Cloke, F. G. N. *J. Org. Chem.* **2008**, *73*, 1076.

(5) Gomes, L. F. R.; Trindade, A. F.; Candeias, N. R.; Gois, P. M. P.; Afonso, C. A. M. *Tetrahedron Lett.* **2009**, *49*, 7372.

(6) (a) Hahn, F. E. *Angew. Chem. Int. Ed.* **2006**, *45*, 1348. (b) Herrmann, W. A. *Angew. Chem. Int. Ed.* **2002**, *41*, 1290. (c) *N-Heterocyclic Carbenes in Transition Metal Catalysis*; Glorius, F., Ed.; Springer: Berlin, **2007**. (d) *N-Heterocyclic Carbenes in Synthesis*; Nolan, S. P., Ed.; Wiley-VCH: Weinheim, **2006**.

(7) Snyder, J. P.; Padwa, A.; Stengel, T.; Arduengo, A. J. III.; Jockisch, A.; Kim, H.-L. *J. Am. Chem. Soc.* **2001**, *123*, 11318.

(8) (a) Parr, R. G.; Yang, W. *Density Functional Theory of Atoms and Molecules*; Oxford University Press: New York, **1989**. (b) The calculations were performed by using the GAUSSIAN 98 package at the B3LYP/VDZP level for all molecules except **6′**, where the B3PW91 functional was used. A full account of the computational details and a complete list of references are provided as Supporting Information.

(9) Candeias, N. R.; Gois, P. M. P.; Veiros, L. F.; Afonso, C. A. M. *J. Org. Chem.* **2008**, *73*, 3539.

(10) Candeias, N. R.; Gois, P. M. P.; Afonso, C. A. M. *J. Org. Chem.* **2006**, *71*, 5489.

(11) Gois, P. M. P.; Afonso, C. A. M. *Eur. J. Org. Chem.* **2003**, 3798.

(12) Yoon, C. H.; Zaworotko, M. J.; Moulton, B.; Jung, K. W. *Org. Lett.* **2001**, *3* , 3539.

(13) Arduengo, A. J. III.; Krafczyk, R.; Schmutzler, R.; Craig, H. A.; Goerlich, J. R.; Marshall, W. J.; Unverzagt, M. *Tetrahedron* **1999**, *55*, 14523.

(14) Deyrup, J. A.; Moyer, C. L. *J. Org. Chem.* **1969**, *34*, 175.

(15) Doyle, M. P.; Westrum, L. J.; Wolthuis, W. N. E.; See, M. M.; Boone, W. P.; Bagheri, V.; Pearson, M. M. *J. Am. Chem. Soc.* **1993**, *115*, 958.

(16) Anada, M.; Hashimoto, S. *Tetrahedron Lett.* **1998**, *39*, 79.

(17) Wee, A. G. H.; Duncan, S. C. *J. Org. Chem.* **2005**, *70*, 8372.